

Two-Fold C–H/C–H Cross-Coupling Using $\text{RhCl}_3 \cdot 3\text{H}_2\text{O}$ as the Catalyst: Direct Fusion of *N*-(Hetero)arylimidazolium Salts and (Hetero)arenes

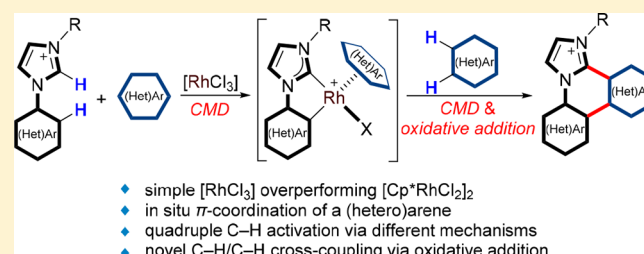
Zhijie She,^{†,‡} Yi Wang,^{‡,‡} Deping Wang,[†] Yinsong Zhao,[†] Tianbao Wang,[†] Xuesong Zheng,[†] Zhi-Xiang Yu,^{*,‡} Ge Gao,^{*,‡} and Jingsong You^{*,†}

[†]Key Laboratory of Green Chemistry and Technology of Ministry of Education, College of Chemistry, Sichuan University, 29 Wangjiang Road, Chengdu 610064, PR China

[‡]Beijing National Laboratory for Molecular Sciences (BNLMS), Key Laboratory of Bioorganic Chemistry and Molecular Engineering of Ministry of Education, College of Chemistry, Peking University, Beijing 100871, China

Supporting Information

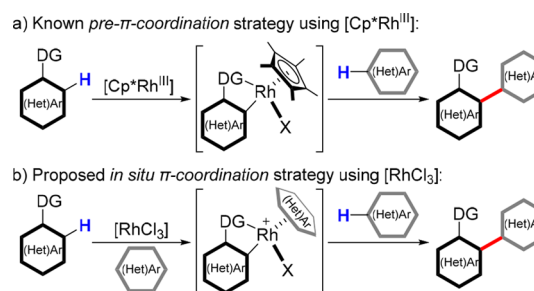
ABSTRACT: $[\text{Cp}^*\text{RhCl}_2]_2$ is the most prevailing catalyst employed for rhodium-catalyzed chelation-assisted C–H/C–H cross-coupling reactions due to the special ligand effect of Cp^* . In this article, a novel concept of using a simple inorganic rhodium salt, $\text{RhCl}_3 \cdot 3\text{H}_2\text{O}$, as the catalyst by taking advantage of in situ π -coordination to Rh with a (hetero)-aromatic reaction component to stabilize Rh intermediates is proposed and evaluated. Our studies not only prove the feasibility of this concept but also disclose a novel 2-fold C–H/C–H cross-coupling reaction of *N*-(hetero)-arylimidazolium salts with various (hetero)arenes to access water-soluble, fluorescent, cationic, and planar polycyclic heteroaromatic molecules, in which $\text{RhCl}_3 \cdot 3\text{H}_2\text{O}$ outperforms $[\text{Cp}^*\text{RhCl}_2]_2$. Mechanistic experiments and DFT calculations reveal that this successive quadruple C–H activation reaction consists of two different C–H activation modes, i.e., concerted metalation–deprotonation (CMD) and oxidative addition. Notably, this is the first report of a C–H bond activation via oxidative addition to Rh^{I} in a bi(hetero)aryl formation with hydrogen evolution. Finally, the different ligand electrochemical parameters of neutral (hetero)arenes and anionic Cp^* are used to explain the different catalytic behaviors of $\text{RhCl}_3 \cdot 3\text{H}_2\text{O}$ and $[\text{Cp}^*\text{RhCl}_2]_2$.



INTRODUCTION

Over the past decades, transition-metal-catalyzed C–C bond formation reactions via C–H bond activation have met tremendous development.¹ Direct C–H/C–H cross-coupling of two (hetero)arenes to build bi(hetero)aryl scaffolds is generally considered as an ideal and more step-/atom-economic strategy over the traditional cross-coupling reactions using organometallic reagents and/or organo(pseudo)halides.² In this context, Cp^* -coordinated Rh^{III} complexes ($[\text{Cp}^*\text{Rh}^{\text{III}}]$, e.g., $[\text{Cp}^*\text{RhCl}_2]_2$, $\text{Cp}^* = 1,2,3,4,5$ -pentamethylcyclopentadienyl) have shown great power in chelation-assisted C–H/C–H cross-coupling reactions due to their high efficiency, selectivity, and functional group tolerance (Scheme 1a).^{3,4} The Cp^* ligand is believed to be necessary not only to stabilize organorhodium intermediates via π -coordination but also to facilitate reductive elimination to yield coupling products due to its steric hindrance.^{3,5} $[\text{Cp}^*\text{RhCl}_2]_2$ is generally prepared from the coordination reaction of $\text{RhCl}_3 \cdot 3\text{H}_2\text{O}$ with excess 1,2,3,4,5-pentamethylcyclopentadiene in methanol under an inert atmosphere,⁶ and now is also a commercially available reagent.

Scheme 1. Strategies for the Chelation-Assisted C–H/C–H Cross-Couplings Using $[\text{Cp}^*\text{Rh}^{\text{III}}]$ and $[\text{RhCl}_3]$



Due to the aforementioned reasons, the Rh source to produce $[\text{Cp}^*\text{RhCl}_2]_2$, a simple inorganic salt, $\text{RhCl}_3 \cdot 3\text{H}_2\text{O}$ is seldom considered as a catalyst.⁷ An easily neglected and rarely noticed fact is that neutral (hetero)arenes are also capable of π -coordinating to Rh,⁸ although their coordination is weaker than that of anionic Cp^* . We envisaged that whether $\text{RhCl}_3 \cdot 3\text{H}_2\text{O}$

Received: July 16, 2018

Published: August 31, 2018

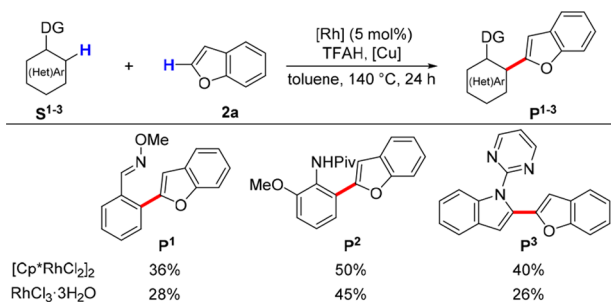
$3\text{H}_2\text{O}$ could be employed directly as the catalyst instead of $[\text{Cp}^*\text{Rh}^{\text{III}}]$ complexes for chelation-assisted C–H/C–H cross-coupling reactions considering that (hetero)arenes could not only serve as a reaction component but also in situ π -coordinate to Rh in the reaction flask to play a similar role to Cp^* ligand (Scheme 1b).

For Rh-catalyzed chelation-assisted C–H/C–H cross-coupling reactions, the majority of C–H bond activation occurs on Rh^{III} via a base-assisted concerted metalation–deprotonation (CMD) mechanism.⁹ Nevertheless, C–H bond activation via oxidative addition to Rh^{I} has never been disclosed in any C–H/C–H cross-coupling reaction to synthesize bi(hetero)aryls.¹⁰ In this article, we would like to present the feasibility of our proposed in situ π -coordination strategy for simple $\text{RhCl}_3 \cdot 3\text{H}_2\text{O}$ -catalyzed C–H/C–H cross-coupling reactions, which leads to the discovery of a novel 2-fold C–H/C–H cross-coupling reaction of *N*-(hetero)arylimidazolium salts with various (hetero)arenes to access polycyclic heteroaromatic molecules. The mechanistic experiments as well as DFT calculations support the proposed strategy and reveal for the first time the C–H bond activation via oxidative addition to Rh^{I} for a C–H/C–H bi(hetero)aryl formation with hydrogen evolution.

RESULTS AND DISCUSSION

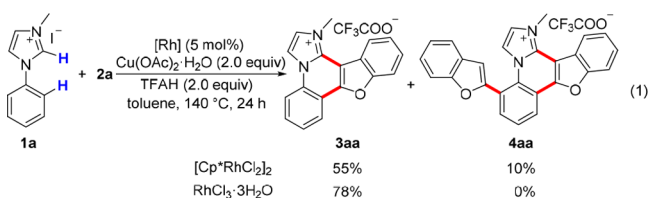
Proof of Concept. To validate the hypothesis, we tentatively subjected three representative substrates, benzaldehyde *O*-methyl oxime¹¹ (**S**¹), *N*-(2-methoxyphenyl)-pivalamide¹² (**S**²), and 1-(pyrimidin-2-yl)-1*H*-indole¹³ (**S**³) to cross-coupling with benzofuran (**2a**) by utilizing $\text{RhCl}_3 \cdot 3\text{H}_2\text{O}$ as the catalyst (Scheme 2). Trifluoroacetic acid (TFAH)

Scheme 2. Comparison of Cross-Couplings of **S^{1–3} with **2a** Catalyzed by $[\text{Cp}^*\text{RhCl}_2]_2$ and $\text{RhCl}_3 \cdot 3\text{H}_2\text{O}$**



was added intentionally to enhance the π -coordination of **2a** toward rhodium.¹⁴ The desired products were delightfully obtained, albeit in slightly lower yields than those in the corresponding $[\text{Cp}^*\text{RhCl}_2]_2$ -catalyzed reactions.

Surprisingly, when 3-methyl-1-phenyl-1*H*-imidazol-3-ium iodide (**1a**) was used as the substrate, the $\text{RhCl}_3 \cdot 3\text{H}_2\text{O}$ -catalyzed reaction afforded a 2-fold C–H/C–H cross-coupling product **3aa** in 78% yield (eq 1). Apparently, **3aa** was formed

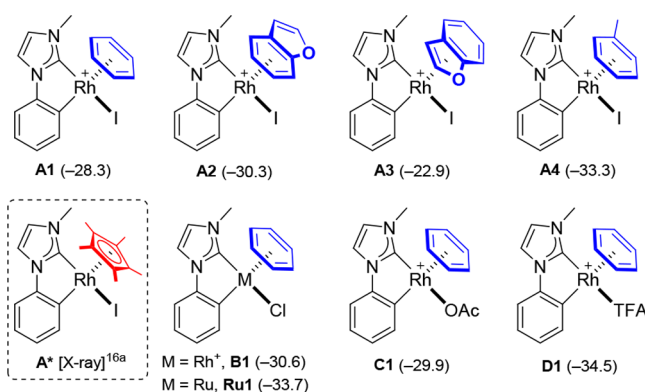


by an *N*-heterocyclic carbene (NHC)-directed cascade inter/intramolecular cross-coupling reaction. However, under the catalysis of $[\text{Cp}^*\text{RhCl}_2]_2$, **3aa** was obtained in a lower yield of 55% inevitably with a small amount of 3-fold C–H/C–H cross-coupling product **4aa** (10%) as a byproduct. The structures of **3aa** and **4aa** were confirmed by ¹H, ¹³C, and ¹⁹F nuclear magnetic resonance (NMR) spectroscopy and high-resolution mass spectrometry (HRMS).

This reaction provides the first example of a direct 2-fold C–H/C–H cross-coupling reaction to build a polycyclic heteroaromatic molecule via quadruple C–H activation.¹⁵ It also combines the first NHC-directed intermolecular C–H/C–H cross-coupling¹⁶ and the first intramolecular C2-heteroarylation of an imidazolium salt with a heteroarene.¹⁷ Most importantly, it demonstrates that the simple inorganic rhodium salt, $\text{RhCl}_3 \cdot 3\text{H}_2\text{O}$, can outperform the prevailing $[\text{Cp}^*\text{RhCl}_2]_2$ in a C–H/C–H cross-coupling reaction with even better selectivity.

Other reaction parameters were also investigated (Tables S1–5). Besides $\text{RhCl}_3 \cdot 3\text{H}_2\text{O}$ and $[\text{Cp}^*\text{RhCl}_2]_2$, other rhodium complexes such as $\text{Cp}^*\text{Rh}(\text{OAc})_2$ and $\text{RhCl}(\text{PPh}_3)_3$ were also workable but gave lower yields. Other transition metal catalysts (e.g., Ru, Pd, Co, and Ir) were inactive. Among the oxidants tested, only copper-based oxidants were compatible, and $\text{Cu}(\text{OAc})_2 \cdot \text{H}_2\text{O}$ was the best. TFAH is so critical that the reaction almost completely ceased with other acidic or basic additives. Moreover, the yield of **3aa** steeply decreased with variation of the reaction temperature. Among the solvents tested, the reaction only proceeded in benzenoid solvents, and toluene provided the highest yield. These results indicated that π -coordinated rhodium intermediates might be in situ generated with benzofuran and/or benzenoid solvents as we proposed (Scheme 1b). We further envisioned that if benzofuran was employed as both a reactant and the solvent then the organorhodium intermediates would also be effectively stabilized by benzofuran to facilitate the coupling reaction to occur. As anticipated, when the reaction was performed in benzofuran for 10 h, **3aa** was obtained in 67% yield, which is lower than that obtained with toluene as the solvent.¹⁸ Finally, the optimal conditions were set to 5 mol % $\text{RhCl}_3 \cdot 3\text{H}_2\text{O}$, 2 equiv of $\text{Cu}(\text{OAc})_2 \cdot \text{H}_2\text{O}$, and 2 equiv of TFAH in toluene at 140 °C for 24 h, and **3aa** was obtained in 78% yield.

To support the feasibility of the in situ π -coordination of (hetero)arenes, DFT calculations were performed to compute the structures and energetics of some possible reaction intermediates (Chart 1). First, benzene was chosen as a representative example of (hetero)arenes (it was also used as a solvent, see Table S5, entry 6). DFT calculations indicated that benzene generates 18-electron intermediate **A1** in a manner similar to that of its counterpart **A*** with anionic Cp^* ligand.^{16a} Benzofuran favors η^6 -coordination (**A2**) to Rh^{III} over the η^5 -one (**A3**) by 7.4 kcal/mol.¹⁹ In addition, the π -coordination energy of benzofuran in **A2** (–30.3 kcal/mol) is between those of benzene in **A1** (–28.3 kcal/mol) and toluene in **A4** (–33.3 kcal/mol). Among rhodium–benzene complexes **A1**–**D1** with different anionic ligands (I^- , Cl^- , OAc^- , and TFA^- , respectively), trifluoroacetate **D1** possesses the strongest π -coordination, confirming that the TFA^- could enhance the π -coordination of (hetero)arenes toward Rh^{III} .¹⁴ Finally, the feasibility of the in situ π -coordination of (hetero)arenes to Rh^{III} was further supported by the similar metal–benzene coordination energies of **B1** (–30.6 kcal/mol) and its

Chart 1. Computed Gibbs Energies for π -Coordination of (Hetero)arenes^a

^aComputed at the M06-D3/def2-TZVPP//M06/def2-SVP level in the gas phase. Reported in kcal/mol.

isoelectronic Ru^{II} counterpart **Ru1** (−33.7 kcal/mol), which is a model complex of the fully characterized [(*p*-cymene)Ru^{II}] complexes.²⁰

In order to capture the possible Rh intermediates, the reactions of **1a** and **2a** in the presence of a stoichiometric amount of RhCl₃·3H₂O and 2 equiv of TFAH were conducted at both room temperature and 140 °C for 2 h. However, no Rh complex could be isolated for characterization. Fortunately, the MALDI–TOF–MS analysis of the mixture of the standard reaction for 2 h showed a peak at *m/z* = 490.996 (Figure 1),

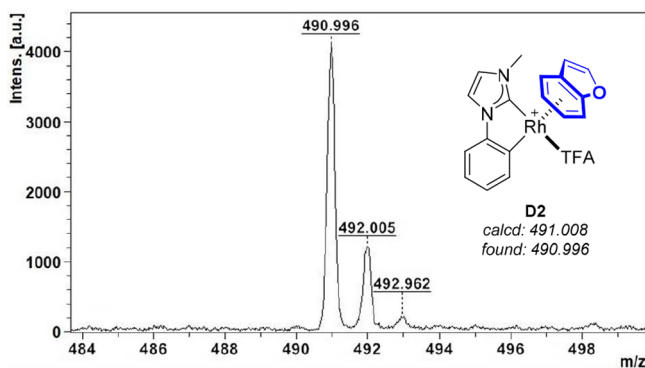
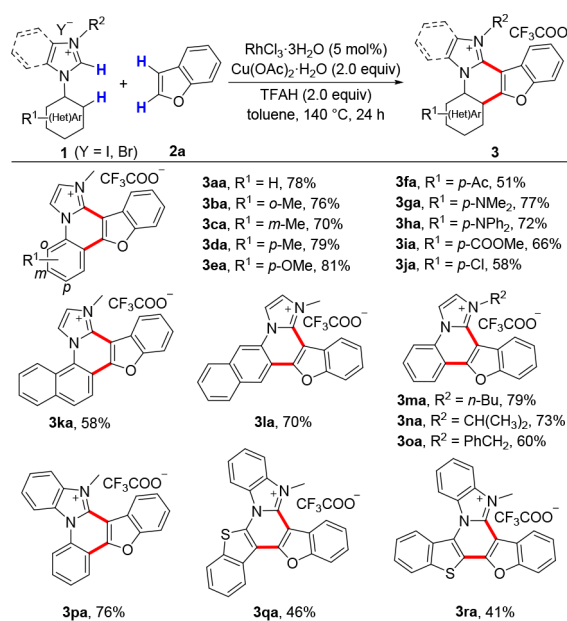


Figure 1. MALDI–TOF–MS analysis of a possible Rh intermediate **D2** obtained from the reaction of **1a** and **2a** under the optimal conditions for 2 h.

which matched the structure of proposed Rh intermediate **D2** (calcd mass: 491.008). Also noted is that no similar Rh intermediate could be captured in the absence of TFAH, indicating its crucial role in stabilizing the Rh intermediates.¹⁴ These experimental results suggest that complex **D2** could possibly be one of the actual Rh intermediates in this reaction. However, the participation of a similar toluene π -coordinated Rh intermediate (**D4**) could not be completely ruled out at the current stage.

Substrate Scope. The reaction scope with respect to *N*-(hetero)arylimidazolium salts was explored under the optimal conditions (Scheme 3). Various functional groups at the *o*/*m*/*p*-positions of the phenyl ring such as methyl, methoxy, acetyl, dimethylamino, and ester groups were well-tolerated, and the corresponding products were isolated in moderate to excellent yields (**3aa–3ia**). Chloro-substituted product **3ja** could be

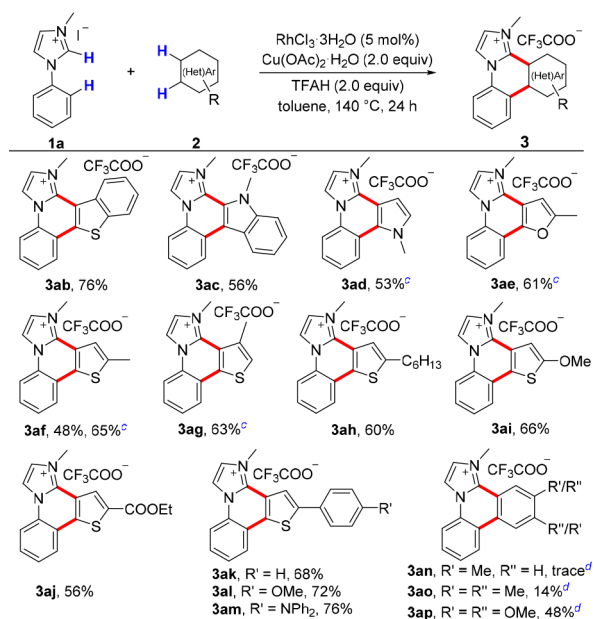
Scheme 3. Scope of Imidazolium Salts^{a,b}

^aReaction conditions: **1** (0.2 mmol), **2a** (0.4 mmol), RhCl₃·3H₂O (5 mol %), Cu(OAc)₂·H₂O (2.0 equiv), and TFAH (2.0 equiv) in toluene (1.0 mL) at 140 °C for 24 h under N₂. ^bIsolated yield.

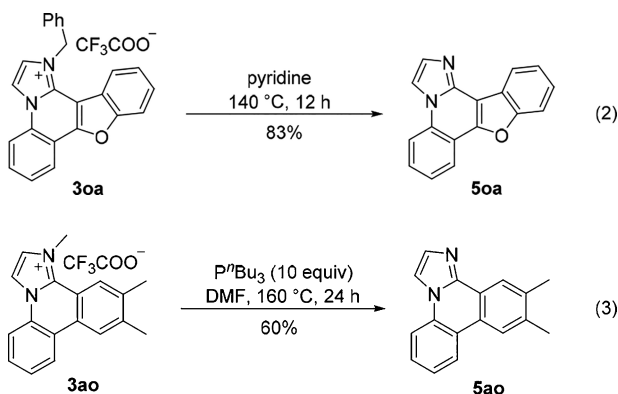
obtained in 58% yield, while significant debromination was observed for a bromo-substituted substrate. The bulky 1-naphthyl substituent led to a lower yield of 58% (**3ka**). When 2-naphthyl substrate **1l** was used, the coupling occurred at the 3-position to give **3la** in 70% yield. Besides the methyl group, imidazolium salts with other *N*-alkyl substituents could also be successfully fused (**3ma–3oa**). Notably, this protocol was also applicable to heteroarylimidazolium salts. *N*-(2-Benzothiophenyl) and *N*-(3-benzothiophenyl) benzimidazolium salts furnished the corresponding cationic propellers **3qa** and **3ra** in 46 and 41% yields, respectively.

As depicted in Scheme 4, a variety of heteroarenes including benzothiofene (**2b**), *N*-methylindole (**2c**), *N*-methylpyrrole (**2d**), 2-methylfuran (**2e**), and thiophenes (**2f–m**) were all suitable substrates. Alkoxy, ester, and amino groups were well-tolerated. It is noted that the regioselectivity for the NHC-directed C–H/C–H cross-couplings of the phenyl ring with heteroarenes occurred commonly at the C2-positions of furan, thiophenes, and pyrrole and at the C3-position of indole (**3ab–3am**).²⁴ Although the reaction using toluene (**2n**) as both the reactant and solvent only afforded a trace amount of **3an** at higher temperature of 150 °C, the reactions employing *o*-xylene (**2o**) and *o*-dimethoxybenzene (**2p**) provided corresponding products **3ao** and **3ap** in 14 and 48% yields, respectively. It should be noted that the in situ π -coordinated Rh^{III} intermediate with **2p** was also captured by the MALDI–TOF–MS analysis (Figure S1).

Polycyclic heteroaromatic products **3** feature a planar and cationic triheteroarylene core with fluorescence in water, which could be applied as DNA intercalators.²¹ Moreover, the corresponding neutral molecules could be obtained by the dealkylation of **3**. For example, debenylation of **3oa** with pyridine furnished **5oa** in 83% yield (eq 2), and demethylation product **5ao** was generated from the reaction of **3ao** with tributylphosphine in 60% yield (eq 3).

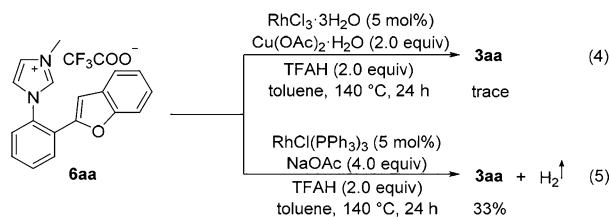
Scheme 4. Scope of (Hetero)arenes^{a,b}

^aReaction conditions: **1a** (0.2 mmol), **2** (0.4 mmol), $\text{RhCl}_3 \cdot 3\text{H}_2\text{O}$ (5 mol %), $\text{Cu}(\text{OAc})_2 \cdot \text{H}_2\text{O}$ (2.0 equiv), and TFAH (2.0 equiv) in toluene (1.0 mL) at 140 °C for 24 h under N₂. ^bIsolated yield. ^c2 (0.6 mmol). ^d2 (1.0 mL as solvent) at 150 °C.



Mechanistic Studies. At first glance, the reaction seems like a 2-fold C–H/C–H cross-coupling via two successive typical Rh^{III}–Rh^I–Rh^{III} cycles (Figure 2, cycle I). On the basis of previous reports,^{9,16} the first two C–H activations of **1a** plausibly occur via CMD to form Rh^{III} intermediates **A–D**. The C2–H activation of **2a** then takes place on the Rh^{III} center, leading to intermediate **E**. Reductive elimination of **E** accomplishes the first C–C bond formation and forms a Rh^I species **F**, which is then oxidized by the Cu^{II} salt to generate Rh^{III} species **G**. The subsequent CMD of the C3–H bond of the benzofuranyl moiety followed by reductive elimination results in the second C–C bond formation, affording final product **3aa** and releases a Rh^I species, which is oxidized by the Cu^{II} salt to regenerate the Rh^{III} catalyst. To judge this mechanism, imidazolium salt **6aa** was synthesized²² and treated under the optimal conditions (in the absence of **2a**). However, expected product **3aa** could only be detected in a trace amount (eq 4), ruling out this pathway.

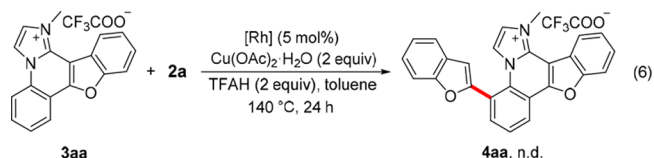
Another possible pathway involves the C3–H bond activation of the benzofuranyl group in **F** via direct oxidative addition to Rh^I, leading to a Rh^{III} intermediate **I** (Figure 2,



cycle II). To verify this hypothesis, DFT calculations were performed on the reaction of simplified model intermediate **D1** with **2a** (Figure 3).^{23,24} The reaction begins with the formation of 18-electron Rh^{III} intermediate **COM1** (benzene and **2a** are η¹- and η²-coordinated, respectively), which undergoes the C2 metalation of **2a** via 16-electron CMD transition state **TS1** (benzene and **2a** are η²- and η¹-coordinated, respectively).²⁵ Resulting intermediate **E1** accomplishes the first C–C bond formation via reductive elimination transition state **TS2**, generating 18-electron Rh^I intermediate **F1**. Then, **F1** undergoes an oxidative addition to form a Rh^{III}–H complex **I1** via **TS3** with an activation Gibbs energy of 26.1 kcal/mol. Subsequently, the second C–C bond formation occurs via reductive elimination transition state **TS4** with an overall activation Gibbs energy of 31.9 kcal/mol (from **F1** to **TS4**), generating **3aa**–Rh^I–H complex **J1**. Finally, the reaction of **J1** with TFAH releases product **3aa**, hydrogen gas, and a Rh^I–benzene complex, which is then oxidized by the Cu^{II} salt to regenerate the Rh^{III} catalyst. It is noteworthy that the transformation of **F1** into **J1** is endergonic and thus requires to be combined with an exergonic hydrogen evolution process to complete the catalytic cycle, which is the reason why a strong acidic environment is necessary for this reaction (Table S3 and eqs S5–S8).

According to these computational results, the intramolecular C–H/C–H coupling of **6aa** might produce **3aa** with hydrogen evolution under the catalysis of a Rh^I catalyst in the absence of any oxidant (Figure 3, dashed). To our delight, **3aa** was isolated in 33% yield by employing RhCl(PPh₃)₃ as the catalyst (eq 5). Hydrogen gas was also detected by GC in a large-scale reaction (see the Supporting Information). To the best of our knowledge, this transformation represents the first example of bi(hetero)aryl formation via a Rh^I-catalyzed C–H/C–H cross-reaction with hydrogen evolution.

Ligand Effect on the Selectivity. To rationalize the different catalytic behaviors of [Cp^{*}RhCl₂]₂ and RhCl₃·3H₂O in this C–H/C–H cross-coupling reaction (eq 1), we conducted a series of control experiments. First, the reaction of **3aa** with **2a** under rhodium catalysis did not lead to the formation of the 3-fold C–H/C–H cross-coupling product **4aa**, while **3aa** was fully recovered (eq 6): This result precluded the possibility of an abnormal N-heterocyclic carbene (aNHC)-directed C–H/C–H cross-coupling after **3aa** was formed.^{16b–d}



Furthermore, the stoichiometric experiments of the [Cp^{*}Rh^{III}] complex **A*** with **2a** provided **4aa** only in the presence of Cu(OAc)₂·H₂O (eq 7), indicating that its

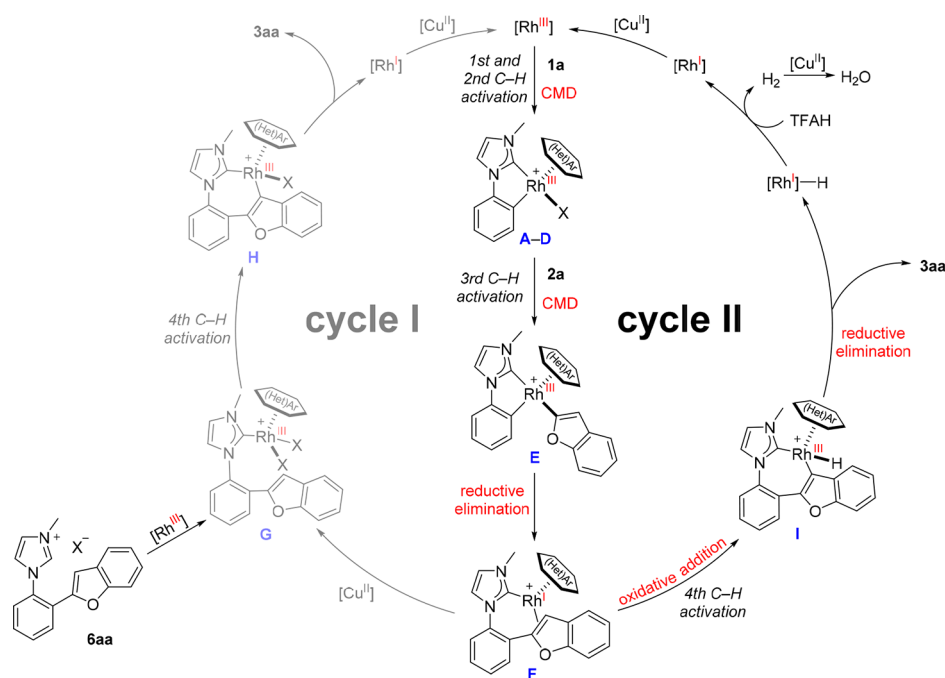


Figure 2. Possible reaction mechanisms. Ligands are not fully shown in some intermediates for clarity. X = I, Cl, OAc, TFA.

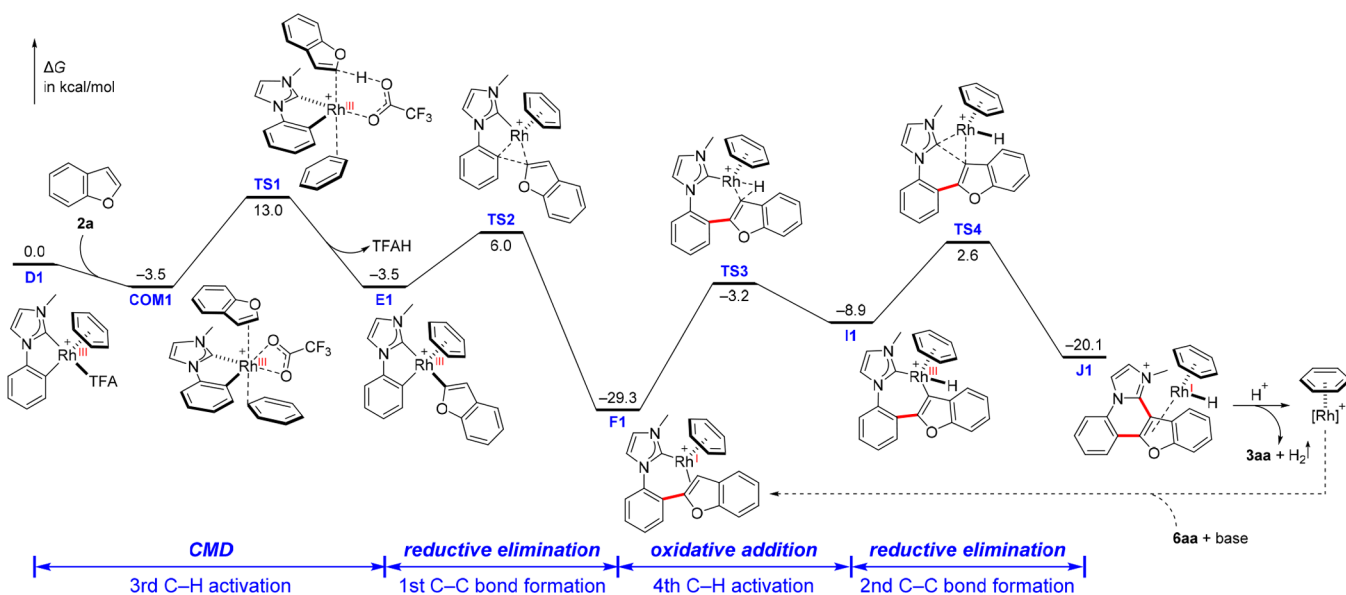
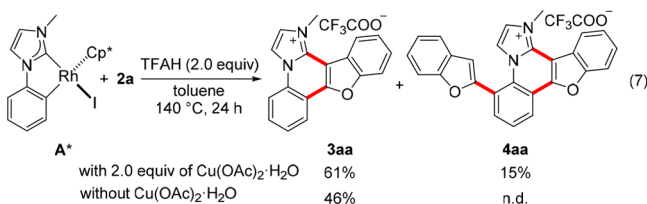


Figure 3. Gibbs energy profile for the two successive C–C bond formations. Computed at the SMD(toluene)/M06-D3/def2-TZVPP//M06/def2-SVP level.

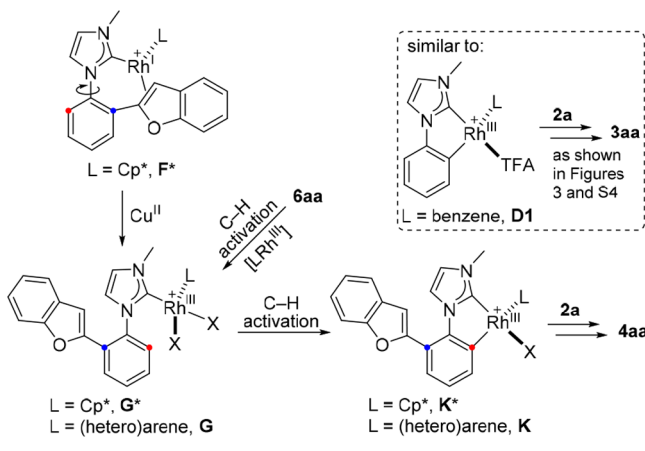


formation might originate from oxidation of Rh^I intermediate F* by the Cu^{II} salt (Scheme 5). A reasonable explanation is that a portion of F* was oxidized by the Cu^{II} salt into Rh^{III} intermediate G*. Then, G* underwent an NHC-directed *ortho* C–H bond activation on the phenyl ring to generate K*, which was then transformed into 4aa via a similar pathway

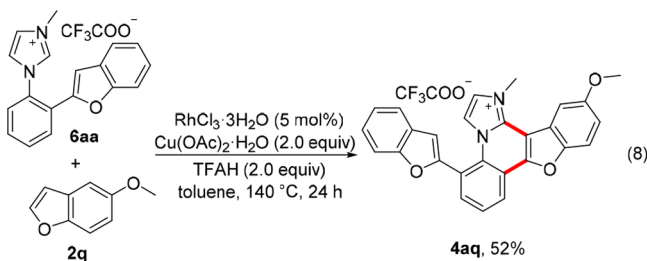
from D1 to 3aa as depicted in Figure 3 (see also Figure S4). When RhCl₃·3H₂O was employed as the catalyst, however, the transformation of F into I via oxidative addition completely suppressed the oxidation of F into G by the Cu^{II} salt, providing 3aa as the only product without 4aa.

The blocked pathway of the oxidation of F with the Cu^{II} salt probably stems from the lower oxidizability of (hetero)arene-coordinated Rh complex F than its Cp* counterpart F*. The much larger Lever's ligand electrochemical parameters (E_L s)²⁶ of neutral (hetero)arenes than anionic Cp* (e.g., $E_L(\text{benzene}) = +1.86 \text{ V}$, $E_L(\text{Cp}^*) = \text{ca. } 0 \text{ V}$) indicate the higher oxidation potential of F than F*. It is also in line with the frontier molecular orbital (FMO) analysis that the HOMO energy of F1 (−9.0 eV) is lower than that of F* (−4.3 eV).

Scheme 5. Rationalization of the Formation of 4aa



Although **G** might not be generated by the oxidation of **F** with the Cu^{II} salt, direct C–H bond activation of **6aa** by $\text{RhCl}_3 \cdot 3\text{H}_2\text{O}$ should be viable taking the 2-benzofuranyl group solely as an intact substituent. As anticipated, the reaction of **6aa** with 5-methoxybenzofuran (**2q**) provided the corresponding 2-fold C–H/C–H cross-coupling product **4aq** in 52% yield (eq 8). This is in support of the proposed mechanism shown in Scheme 5.



CONCLUSIONS

An in situ π -coordination strategy is proposed and evaluated for C–H/C–H cross-coupling reactions using a simple inorganic salt, $\text{RhCl}_3 \cdot 3\text{H}_2\text{O}$, as the catalyst instead of the prevailing $[\text{Cp}^*\text{RhCl}_2]_2$. It is not only proven to be feasible for several selected C–H/C–H cross-coupling reactions but also leads to the discovery of a novel 2-fold C–H/C–H cross-coupling reaction of *N*-(hetero)arylimidazolium salts with (hetero)arenes via quadruple C–H bond activation. This reaction has a broad substrate scope and delivers various cationic polycyclic heteroaromatic molecules, which can also be easily transformed into neutral ones. The interesting photophysical properties as well as applications of these water-soluble, fluorescent, cationic, and planar triheteroarylene analogues are currently under investigation in our laboratory. Mechanistic experiments and DFT calculations reveal that (hetero)arenes in situ η^6 -coordinated to Rh^{III} to stabilize the organorhodium intermediates in this reaction in a similar manner to $[\text{Cp}^*\text{Rh}^{\text{III}}]$ complexes as we proposed. More interestingly, the first C–H/C–H cross-coupling goes through a typical $\text{Rh}^{\text{III}}-\text{Rh}^{\text{I}}$ process, while the second one undergoes an unprecedented $\text{Rh}^{\text{I}}-\text{Rh}^{\text{III}}-\text{Rh}^{\text{I}}$ cycle with hydrogen evolution. The crucial role of TFAH is not only to facilitate in situ π -coordination of (hetero)arenes to Rh^{III} but also to react with the $\text{Rh}-\text{H}$ species to complete the catalytic cycle. Moreover, the different catalytic behaviors of $\text{RhCl}_3 \cdot 3\text{H}_2\text{O}$ and

$[\text{Cp}^*\text{RhCl}_2]_2$ are attributed to the ligand effect on the redox properties of the reaction intermediates. We envision that this in situ π -coordination strategy would also be applicable to reactions catalyzed by other metals (such as Ir and Co) having structurally similar Cp^* complexes.

EXPERIMENTAL SECTION

Procedure for the $\text{RhCl}_3 \cdot 3\text{H}_2\text{O}$ -Catalyzed Reaction of 1a with 2a. A flame-dried Schlenk test tube with a magnetic stirring bar was charged with 3-methyl-1-phenyl-1*H*-imidazol-3-ium iodide (**1a**) (57.2 mg, 0.2 mmol), benzofuran (**2a**) (44.1 μL , 0.4 mmol), $\text{RhCl}_3 \cdot 3\text{H}_2\text{O}$ (2.6 mg, 0.01 mmol), $\text{Cu}(\text{OAc})_2 \cdot \text{H}_2\text{O}$ (79.9 mg, 0.4 mmol), TFAH (29.7 μL , 0.4 mmol), and toluene (1.0 mL) under a N_2 atmosphere. The reaction mixture was stirred for 5 min at room temperature and then heated at 140 $^\circ\text{C}$ for 24 h. The reaction solution was cooled down to ambient temperature, diluted with 10 mL of CH_2Cl_2 , filtered through a Celite pad, and washed with 10–20 mL of CH_2Cl_2 . The combined organic extracts were then concentrated, and the resulting residue was purified by column chromatography on silica gel with $\text{CH}_2\text{Cl}_2/\text{MeOH}$ (v/v, 20/1) to provide 60.2 mg of **3aa** as a white solid in 78% yield. Mp 218–220 $^\circ\text{C}$. ^1H NMR (400 MHz, $\text{DMSO}-d_6$) δ = 4.58 (s, 3H), 7.56 (t, J = 8.0 Hz, 1H), 7.67 (t, J = 8.4 Hz, 1H), 7.89 (t, J = 7.6 Hz, 1H), 7.93 (d, J = 8.4 Hz, 1H), 8.04 (t, J = 8.8 Hz, 1H), 8.36 (d, J = 2.4 Hz, 1H), 8.40 (d, J = 9.2 Hz, 1H), 8.44 (d, J = 8.0 Hz, 1H), 8.70 (d, J = 8.8 Hz, 1H), 9.19 (d, J = 2.4 Hz, 1H) ppm. ^{13}C NMR (100 MHz, $\text{DMSO}-d_6$) δ = 38.2, 104.2, 112.8, 113.5, 114.5, 117.4, 120.2, 122.9, 123.5, 125.4, 126.2, 128.4, 128.6, 130.6, 132.4, 136.8, 153.6, 155.3 ppm. ^{19}F NMR (376 MHz, $\text{DMSO}-d_6$) δ = –73.55 ppm. HRMS (ESI $^+$) calcd for $\text{C}_{18}\text{H}_{13}\text{N}_2\text{O}^+ [\text{M} - \text{CF}_3\text{COO}^-]^+$ 273.1022, found 273.1019.

Computational Methods. DFT calculations were performed with Gaussian 09.²⁷ Pruned integration grids with 99 radial shells and 590 angular points per shell were used. Geometry optimizations of the stationary points were carried out at the M06²⁸/def2-SVP²⁹ level without any constraints. Unscaled harmonic frequency calculations at the same level were performed to validate each structure as either a minimum or a transition state and to evaluate its zero-point energy and thermal corrections at 298 K. Quasiharmonic corrections were applied during the entropy calculations by setting all positive frequencies that are less than 100 cm^{-1} to 100 cm^{-1} .³⁰ On the basis of the optimized structures, single-point energies were computed at the M06-D3/def2-TZVPP level.^{28,29,31} Gibbs energies of solvation in toluene were obtained at the same level using the SMD solvation model.³² All discussed energy differences were based on Gibbs energies at 298 K unless otherwise specified. Standard states for gases and solutes in toluene solution are the hypothetical states at 1 atm and 1 mol/L, respectively. Orbital energies were computed at the M06/def2-SVP level.

ASSOCIATED CONTENT

Supporting Information

The Supporting Information is available free of charge on the ACS Publications website at DOI: 10.1021/jacs.8b07485.

Experimental procedures, characterization data, copies of NMR spectra, and additional computational results (PDF)

AUTHOR INFORMATION

Corresponding Authors

*E-mail: gg2b@scu.edu.cn.

*E-mail: jsyou@scu.edu.cn.

*E-mail: yuwx@pku.edu.cn.

ORCID

Yi Wang: 0000-0001-5762-5958

Zhi-Xiang Yu: 0000-0003-0939-9727

Ge Gao: 0000-0001-9980-7311

Jingsong You: 0000-0002-0493-2388

Author Contributions

#Z.S. and Y.W. contributed equally.

Notes

The authors declare no competing financial interest.

ACKNOWLEDGMENTS

We thank the National Natural Science Foundation of China (Nos. 21472127, 21772134, 21232001, and 21432005) and the Graduate Student's Research and Innovation Fund of Sichuan University (No. 2018YJSY052) for financial support.

REFERENCES

- (1) For selected reviews, see (a) Yeung, C. S.; Dong, V. M. *Chem. Rev.* **2011**, *111*, 1215. (b) Yamaguchi, J.; Yamaguchi, A. D.; Itami, K. *Angew. Chem., Int. Ed.* **2012**, *51*, 8960. (c) Liu, C.; Yuan, J.; Gao, M.; Tang, S.; Li, W.; Shi, R.; Lei, A. *Chem. Rev.* **2015**, *115*, 12138.
- (2) For selected reviews, see (a) Bugaut, X.; Glorius, F. *Angew. Chem., Int. Ed.* **2011**, *50*, 7479. (b) Zhao, D.; You, J.; Hu, C. *Chem. - Eur. J.* **2011**, *17*, 5466. (c) Cho, S. H.; Kim, J. Y.; Kwak, J.; Chang, S. *Chem. Soc. Rev.* **2011**, *40*, 5068. (d) Yang, Y.; Lan, J.; You, J. *Chem. Rev.* **2017**, *117*, 8787.
- (3) For selected reviews, see (a) Satoh, T.; Miura, M. *Chem. - Eur. J.* **2010**, *16*, 11212. (b) Colby, D. A.; Tsai, A. S.; Bergman, R. G.; Ellman, J. A. *Acc. Chem. Res.* **2012**, *45*, 814. (c) Song, G.; Wang, F.; Li, X. *Chem. Soc. Rev.* **2012**, *41*, 3651. (d) Song, G.; Li, X. *Acc. Chem. Res.* **2015**, *48*, 1007.
- (4) For representative examples of [Cp*Rh^{III}]-catalyzed C–H/C–H cross-coupling, see (a) Wencel-Delord, J.; Nimphius, C.; Patureau, F. W.; Glorius, F. *Angew. Chem., Int. Ed.* **2012**, *51*, 2247. (b) Morimoto, K.; Itoh, M.; Hirano, K.; Satoh, T.; Shibata, Y.; Tanaka, K.; Miura, M. *Angew. Chem., Int. Ed.* **2012**, *51*, 5359. (c) Kuhl, N.; Hopkinson, M. N.; Glorius, F. *Angew. Chem., Int. Ed.* **2012**, *51*, 8230. (d) Wencel-Delord, J.; Nimphius, C.; Wang, H.; Glorius, F. *Angew. Chem., Int. Ed.* **2012**, *51*, 13001. (e) Dong, J.; Long, Z.; Song, F.; Wu, N.; Guo, Q.; Lan, J.; You, J. *Angew. Chem., Int. Ed.* **2013**, *52*, 580.
- (5) (a) Piou, T.; Romanov-Michailidis, F.; Romanova-Michaelides, M.; Jackson, K. E.; Semakul, N.; Taggart, T. D.; Newell, B. S.; Rithner, C. D.; Paton, R. S.; Rovis, T. *J. Am. Chem. Soc.* **2017**, *139*, 1296. (b) Piou, T.; Rovis, T. *Acc. Chem. Res.* **2018**, *51*, 170.
- (6) (a) Kang, J. W.; Moseley, K.; Maitlis, P. M. *J. Am. Chem. Soc.* **1969**, *91*, 5970. (b) Fujita, K.; Takahashi, Y.; Owaki, M.; Yamamoto, K.; Yamaguchi, R. *Org. Lett.* **2004**, *6*, 2785.
- (7) For randomly selected RhCl₃·3H₂O as the catalyst for C–H bond activation reactions, see (a) Witulski, B.; Schweikert, T. *Synthesis* **2005**, *2005*, 1959. (b) Wang, P.; Rao, H.; Hua, R.; Li, C.-J. *Org. Lett.* **2012**, *14*, 902. (c) Ran, Y.; Yang, Y.; You, H.; You, J. *ACS Catal.* **2018**, *8*, 1796.
- (8) (a) Maekawa, M.; Hashimoto, N.; Kuroda-Sowa, T.; Suenaga, Y.; Munakata, M. *Anal. Sci.* **2001**, *17*, 1361. (b) Muratov, D. V.; Romanov, A. S.; Loginov, D. A.; Corsini, M.; Fabrizi de Biani, F.; Kudinov, A. R. *Eur. J. Inorg. Chem.* **2015**, *2015*, 804.
- (9) (a) Lapointe, D.; Fagnou, K. *Chem. Lett.* **2010**, *39*, 1118. (b) Ackermann, L. *Chem. Rev.* **2011**, *111*, 1315. (c) Davies, D. L.; Macgregor, S. A.; McMullin, C. L. *Chem. Rev.* **2017**, *117*, 8649.
- (10) For examples of rhodium(I)-catalyzed decarbonylative C–H arylation and alkenylation reactions, see (a) Pan, F.; Lei, Z.-Q.; Wang, H.; Li, H.; Sun, J.; Shi, Z.-J. *Angew. Chem., Int. Ed.* **2013**, *52*, 2063. (b) Zhang, L.; Qiu, R.; Xue, X.; Pan, Y.; Xu, C.; Wang, D.; Wang, X.; Xu, L.; Li, H. *Chem. Commun.* **2014**, *50*, 12385.
- (11) Qin, D.; Wang, J.; Qin, X.; Wang, C.; Gao, G.; You, J. *Chem. Commun.* **2015**, *51*, 6190.
- (12) Huang, Y.; Wu, D.; Huang, J.; Guo, Q.; Li, J.; You, J. *Angew. Chem., Int. Ed.* **2014**, *53*, 12158.
- (13) Qin, X.; Liu, H.; Qin, D.; Wu, Q.; You, J.; Zhao, D.; Guo, Q.; Huang, X.; Lan, J. *Chem. Sci.* **2013**, *4*, 1964.
- (14) Rybinskaya, M. I.; Kudinov, A. R.; Kaganovich, V. S. *J. Organomet. Chem.* **1983**, *246*, 279.
- (15) (a) Nagao, I.; Shimizu, M.; Hiyama, T. *Angew. Chem., Int. Ed.* **2009**, *48*, 7573. (b) Ozaki, K.; Matsuoka, W.; Ito, H.; Itami, K. *Org. Lett.* **2017**, *19*, 1930. (c) Matsuoka, W.; Ito, H.; Itami, K. *Angew. Chem., Int. Ed.* **2017**, *56*, 12224.
- (16) NHC-directed C–H annulation reactions were reported; see (a) Ghorai, D.; Choudhury, J. *Chem. Commun.* **2014**, *50*, 15159. (b) Ghorai, D.; Choudhury, J. *ACS Catal.* **2015**, *5*, 2692. (c) Li, R.; Hu, Y.; Liu, R.; Hu, R.; Li, B.; Wang, B. *Adv. Synth. Catal.* **2015**, *357*, 3885. (d) Ge, Q.; Li, B.; Wang, B. *Org. Biomol. Chem.* **2016**, *14*, 1814.
- (17) Li, S.; Tang, J.; Zhao, Y.; Jiang, R.; Wang, T.; Gao, G.; You, J. *Chem. Commun.* **2017**, *53*, 3489.
- (18) When *N*-methylpyrrole (**2d**) and 2-methylthiophene (**2f**) were used as both a reactant and the solvent, **3ad** and **3af** were isolated in 58 and 70% yields, respectively. See eqs S2 and S3.
- (19) Similar results have been observed in previous reports; see (a) White, C.; Thompson, S. J.; Maitlis, P. M. *J. Chem. Soc., Dalton Trans.* **1977**, 1654. (b) Polam, J. R.; Porter, L. C. *J. Organomet. Chem.* **1994**, *482*, 1.
- (20) Ma, C.; Ai, C.; Li, Z.; Li, B.; Song, H.; Xu, S.; Wang, B. *Organometallics* **2014**, *33*, 5164.
- (21) Parenty, A. D. C.; Guthrie, K. M.; Song, Y.-F.; Smith, L. V.; Burkholder, E.; Cronin, L. *Chem. Commun.* **2006**, 1194.
- (22) **6aa** was not detected in the reaction of **1a** with **2a**.
- (23) To simplify the computations without sacrificing the understanding of the reaction mechanism, we used the symmetric benzene as the model ligand. If other (hetero)arenes, such as benzofuran and toluene, were used, then hundreds of stationary points (including all the possible conformers) would be located, which is very time-consuming and beyond our ability.
- (24) Due to the significant solvation and counteranion effects on the electrostatic repulsion between the positive charges on the proposed catalyst, [(hetero)arene]RhX₂⁺, and imidazolium cation, the first two C–H activation steps were not considered in our calculations. See the Supporting Information for discussion on the full catalytic cycle based on Cp*.
- (25) To simplify the computations, only TFA[−] was considered in this model reaction. In the real catalytic system, OAc[−] may also participate in the C–H activation steps, and is important for getting better yields according to the control experiments. See the Supporting Information for details.
- (26) Lu, S.; Strelets, V. V.; Ryan, M. F.; Pietro, W. J.; Lever, A. B. P. *Inorg. Chem.* **1996**, *35*, 1013.
- (27) Frisch, M. J.; Trucks, G. W.; Schlegel, H. B.; Scuseria, G. E.; Robb, M. A.; Cheeseman, J. R.; Scalmani, G.; Barone, V.; Mennucci, B.; Petersson, G. A.; Nakatsuji, H.; Caricato, M.; Li, X.; Hratchian, H. P.; Izmaylov, A. F.; Bloino, J.; Zheng, G.; Sonnenberg, J. L.; Hada, M.; Ehara, M.; Toyota, K.; Fukuda, R.; Hasegawa, J.; Ishida, M.; Nakajima, T.; Honda, Y.; Kitao, O.; Nakai, H.; Vreven, T.; Montgomery, J. A., Jr.; Peralta, J. E.; Ogliaro, F.; Bearpark, M.; Heyd, J. J.; Brothers, E.; Kudin, K. N.; Staroverov, V. N.; Keith, T.; Kobayashi, R.; Normand, J.; Raghavachari, K.; Rendell, A.; Burant, J. C.; Iyengar, S. S.; Tomasi, J.; Cossi, M.; Rega, N.; Millam, J. M.; Klene, M.; Knox, J. E.; Cross, J. B.; Bakken, V.; Adamo, C.; Jaramillo, J.; Gomperts, R.; Stratmann, R. E.; Yazyev, O.; Austin, A. J.; Cammi, R.; Pomelli, C.; Ochterski, J. W.; Martin, R. L.; Morokuma, K.; Zakrzewski, V. G.; Voth, G. A.; Salvador, P.; Dannenberg, J. J.; Dapprich, S.; Daniels, A. D.; Farkas, O.; Foresman, J. B.; Ortiz, J. V.; Cioslowski, J.; Fox, D. J. *Gaussian 09*, revision E.01; Gaussian, Inc.: Wallingford, CT, 2013.
- (28) Zhao, Y.; Truhlar, D. G. *Theor. Chem. Acc.* **2008**, *120*, 215.
- (29) Weigend, F.; Ahlrichs, R. *Phys. Chem. Chem. Phys.* **2005**, *7*, 3297.
- (30) (a) Zhao, Y.; Truhlar, D. G. *Phys. Chem. Chem. Phys.* **2008**, *10*, 2813. (b) Ribeiro, R. F.; Marenich, A. V.; Cramer, C. J.; Truhlar, D. G. *J. Phys. Chem. B* **2011**, *115*, 14556.
- (31) Grimme, S.; Antony, J.; Ehrlich, S.; Krieg, H. *J. Chem. Phys.* **2010**, *132*, 154104.

(32) Marenich, A. V.; Cramer, C. J.; Truhlar, D. G. *J. Phys. Chem. B* 2009, 113, 6378.